

Spin correlations in semiconductor dangling bonds: Implications for the alkali-metal-covered surfaces

M. C. Refolio, J. Rubio, M. P. López Sancho, and J. M. López Sancho

Instituto de Ciencia de Materiales de Madrid, Consejo Superior de Investigaciones Científicas, Serrano 144, 28006-Madrid, Spain

(Received 21 July 1993; revised manuscript received 5 October 1993)

It is well known that an antiferromagnetic (AF) spin arrangement within dimers provides a simple explanation of the gap in the electronic structure of the Si(100)-(2×1) reconstructed surface. Taking this AF description at its face value, we explore the implications of strong Si on-site repulsions (U) for the alkali-metal-covered surface in the coverage (θ) range up to two potassium atoms per dimer. As coverage (electron doping) increases, the substrate undergoes an insulator-metal transition which, in contrast with the $U=0$ situation, is gradual and due to weakening and final destruction of the AF ordering and its associated gap. The adsorption bond is strongly ionic in the low-coverage regime, with fractional ionic character (FIC) about 0.9. At $\theta=0.5$ (one-half of the first monolayer), however, a crossover between one-dimensional and two-dimensional behavior is found, with a steep rise of the potassium charge accompanied by a steep drop of the FIC of the bond, both signaling the formation of an occupied potassium band increasingly charged and hybridized with the Si band. This process goes on, but now slowly, along the rest of the coverage range, up to saturation, leading finally to a rather low FIC of the bond (0.28) at $\theta=2$. The above crossover separates the low-coverage regime, insulating and highly ionic, from the high-coverage regime where *both* the substrate and the adsorbate overlayer are metallic and the bonds predominantly covalent. The present model, therefore, does not sustain either the strong ionic picture along the whole coverage range or the opposite view that the transferred charge on the Si atoms is small even at low coverage.

I. INTRODUCTION

The interaction of alkali metals with semiconductor surfaces has been the object of intensive study in recent years due to both its technological applications¹ and the important questions raised by these systems in basic physics.²⁻⁴ The applications range from negative electron-affinity devices, spin-polarized electron-beam sources, and high-yield photoemitters, to the role of alkali metals, as coadsorbates, in promoting important chemical reactions in catalysis. As to basic research, the alkali-metal-semiconductor interface is a nearly ideal model system where several questions, such as, e.g., surface metallization and metal-insulator transitions, can be tested. The nature of these issues depends critically on the character of the alkali-metal-semiconductor bond, which has originated some controversy.

At low coverage, the work function decreases linearly with coverage and the electrons flow from the alkali atoms to the substrate dangling-bond band leading to a large surface dipole. The bond is clearly ionic. As coverage increases, however, the situation ceases to be clear cut, as the nature of the bond may change with increasing coverage. To be specific, let us take the case of the potassium-covered Si(100)-(2×1) surface. Observations of Tochiyama⁵ on this surface seemed to suggest that alkali atoms adsorbed on semiconductor surfaces behave as on metal surfaces. The work function decreases rapidly at submonolayer coverage and, subsequently, after the onset of a 2 eV loss peak, it decreases slowly until completion of the first monolayer ($\theta=1$ K atom per Si dimer) without ever going through a minimum in this range.

The conclusion drawn^{6,7} was just as with transition-metal surfaces.^{8,9} An insulator-metal transition was taking place on the potassium layer below a critical K-K interatomic distance, with a concomitant retransfer of charge from the substrate to the K metal band. The Si-K bond becomes, therefore, essentially covalent with only a small fractional ionic character.

Batra and Bagus,¹⁰ on the other hand, proposed a different interpretation based on a theoretical analysis. Their extensive calculations of the charge density, dipole moment, and binding energy for several energy-minimized geometries led them to conclude that the alkali adsorption on semiconductor surfaces was drastically different from adsorption on metals, due to the presence of active surface dangling bonds on the former. These lead to a large alkali-substrate interaction energy (of some 2.5 eV), considerably larger than the cohesive energy per atom of bulk potassium (0.6 eV). Consequently, the system gains energy by filling the dangling bonds with the K electrons. Thus, the K-Si bond remains ionic and strong as for low coverage. It is the antibonding dangling-bond band that gets half filled, and therefore metallic, without any need of invoking a Mott insulator-metal transition. This conclusion is shared by other authors,¹¹⁻¹³ although arriving at rather different results for the K-Si charge transfer, which they find smaller (0.25–0.50 electrons per K).

Upon further K deposition, a saturation coverage of two atoms per dimer is attained¹⁴ while the work function decreases, going through a minimum somewhat above $\theta=1$,¹⁵ and finally increasing slowly up to a value of 3.2 eV.¹⁴ The interface now seems to be insulating

again.¹⁴ Although this has been called into question by recent spectroscopic measurements,^{16–18} the existence of a gap of about 1 eV between the silicon band and the main potassium band, even at $\theta=2$, seems rather clear.¹⁹ By this $\theta=2$ coverage, the interface appears to be fully developed, since further layers of K deposition do not produce any changes in either work function or spectral features.^{14,15} The explanation offered by Batra²⁰ is very simple and appealing: With two K atoms per dimer, the K electrons flow entirely onto the Si dangling bonds, thereby filling the antibonding dangling-bond band. The Si-K bond remains ionic and strong along the entire coverage range.

The precise nature of the interface metallization is thus still unsettled, as no general agreement has been reached about the ionic versus covalent character of the adsorption bond. Depending on this character, the metallization of the interface may go on via substrate^{10,20} or adlayer^{5–7,11–13} metallization, respectively. Recent experiments,^{16–19,21,22} which will be analyzed in this paper, should help to resolve this conflict. Which of these two pictures turns out to better reflect physical reality is important not only for this problem, but also for its implications on such outstanding topics as, e.g., the catalytic oxidation of alkali-covered silicon surfaces.

Although most of these issues might appear to find a simple explanation in terms of conventional band theory,^{10–13,20} it should be kept in mind that both the geometric and electronic properties of the clean Si(100)-(2×1) surface still remain unclear. For instance, photoemission and inverse photoemission²³ show a semiconducting surface in contrast with the metallic character predicted by early calculations for symmetric dimer arrangements. Despite the tight-binding calculation of Chadi,²⁴ showing a gap of 0.6 eV when the dimers were allowed to buckle, this gap disappeared as soon as self-consistency was introduced. Indeed different self-consistent spin-independent calculations predict a *metallic* surface^{25–27} irrespective of the geometric model used [buckled or nonbuckled dimers, or even a $c(4\times 2)$ reconstruction].²⁶ Simply, the reported absolute gaps are too small (<0.1 eV) against the experimental value of 0.7 eV.²³ Even the recent calculation by Dabrowski and Scheffler²⁷ gives an almost invisible gap. The shape of the bands is generally in fair agreement with the experimental data, but the occupied dangling-bond band is about 0.5 eV above the experimental one.^{25–27}

This is likely a consequence of the local-density approximation (LDA). Gaps can, of course, be obtained within the framework of density-functional theory provided strong local-field corrections are included in the single-particle self-energy. This is the case, e.g., of the recent calculations for the Si(111) surface carried out by Northrup, Hybertsen, and Louie²⁸ within the generalized (exchange-corrected) random-phase approximation (GRPA) for the electron self-energy.²⁹ The price one pays, however, is that the physics tends to be somewhat buried under the fine details of a rather involved formalism. If strong local-field corrections are to be accounted for, it is perhaps better to resort to model Hamiltonians incorporating local electron correlations from the outset,

such as, e.g., the Hubbard Hamiltonian. We shall, therefore, follow this path for simplicity in spite of quite successful recent attempts to incorporate Hubbard-type interactions within a LDA context, the so-called LDA + U formalism.³⁰ The situation of these surfaces, in this respect, is reminiscent of a similar situation with many transition-metal oxides. In the copper oxides, for instance, strong local correlations on the copper sites must be considered, at least within the framework of the Hubbard model, in order to explain their insulating behavior. In the present case, where the dangling-bond bands are indeed very narrow (~ 0.5 eV), quite modest Hubbard U values of 1–2 eV can take us into the intermediate-to-strong correlation limit.

In this connection, cluster calculations³¹ reveal that spin correlations can be of paramount importance for this surface and, on the other hand, spin-resolved nonparametrized calculations by Artacho and Yndurain,³² which consider the on-site interactions in *both* symmetric and asymmetric dimers, show that an antiferromagnetic (AF) spin arrangement within the dimers lowers the total energy and opens an AF gap in the surface band structure. The surface is then always semiconducting, irrespective of the dimer model, while the AF energy lowering (~ 1 eV per dimer) strongly outweighs any energy differences due to different geometric models. Thus, whatever the dimer model adopted AF spin correlations seem *essential* to explain the electronic structure of this surface.

In the present work we take this AF description of the clean surface at its face value and explore the implications of strong on-site Si repulsions for the potassium-covered Si(100)-(2×1) reconstructed system in the coverage range up to two potassium atoms per dimer. We shall discuss general trends and will not aim at quantitative estimates of model-dependent quantities such as charge transfer or Fermi-level shift, which would demand an accurate calculation based on a more realistic model. We shall use them as a general guide for a qualitative discussion of bonding and metallization, stressing some salient features which we believe are model independent. We shall further adopt, for simplicity's sake, the *symmetric* dimer model in this paper (even at very low coverage), in spite of recent low-temperature experiments^{33,34} clearly supporting buckled-dimer domains of $c(4\times 2)$ order. We argue below (Secs. IV and V) that nonbuckled dimers contain the essential ingredients for a theoretical analysis of the alkali-covered surface. In the spirit of the preceding paragraph, Si on-site repulsions *must* be included in any case. Our results should also apply to other surface geometries as well as to other alkali adsorbates.

In a previous paper³⁵ we explored this system under the assumption of very high U/B , B being the Si bandwidth. Since the upper Hubbard band is then risen into the alkali s -band region, the problem was treated as an Anderson-lattice model within a Green-function formalism. Now we describe the surface by a single-orbital (two-band) Hubbard Hamiltonian, which is coupled to a potassium layer. The insulator-to-metal transition is then tied to the special properties of the electron-doped Hubbard model, and may be immediately related to the simi-

lar behavior of the hole-doped CuO_2 conducting planes in the high- T_c superconductors. Some main highlights of this work have been already briefly advanced.³⁶

The Hamiltonian and mean-field formalism used are briefly described in some detail in Sec. II, whereas the simplified model adopted for the interface is given in Sec. III. Section IV is devoted to the initial, very low coverage ($\theta < 0.01$, say), the independent adsorbates limit, where the mechanism of destruction of the AF order is quite neat (the spin and charge bag). The medium (up to $\theta = 1$) and high (the double layer, $1 < \theta < 2$) coverage regimes, where both substrate and adlayer metallization take place, are discussed in Sec. V. A general discussion on bonding and metallization is given in Sec. VI. Some concluding remarks, finally, summarize this paper in Sec. VII.

II. HAMILTONIAN AND MEAN-FIELD FORMALISM

In light of the preceding discussion, we assume the interface to be characterized by the extended Hubbard Hamiltonian

$$H = H_{\text{Si}} + H_{\text{K}} + H_{\text{SiK}} + H_c, \quad (1)$$

where

$$\begin{aligned} H_{\text{Si}} &= - \sum_{\langle ij \rangle_s} t_{ij} c_{is}^+ c_{js} + U \sum_i n_{i\uparrow} n_{i\downarrow}, \\ H_{\text{KK}} &= E_K \sum_{as} n_{as} + \sum_{\langle ab \rangle_s} t_{ab}(\theta) c_{as}^+ c_{bs}, \\ H_{\text{SiK}} &= \sum_{\langle ia \rangle_s} V_{ia} (c_{is}^+ c_{as} + c_{as}^+ c_{is}) \\ &\quad + \sum_{\langle ia \rangle} W_{ia} (n_i - 1)(n_a - 1), \end{aligned}$$

and

$$H_c = E_c \sum_i n_{ic} + W_c \sum_i n_{ic} (n_i - 1). \quad (2)$$

We have retained the standard notation. A two-dimensional array of Si dimers, with intrasite Coulomb repulsions (U) couples through hopping (V) and interatomic Coulomb interactions (W) to a set of potassium atoms that may form a metallic band [$t_{ab}(\theta) \neq 0$ for high enough θ]. The summations over the indices i and a run through all the Si lattice sites and the adsorbate atoms, respectively. In the double sums, the symbol $\langle \rangle$ means summation over first- and second-order neighbors only. Notice that, since the K-Si charge transfer is expected to be large, the W term is essential. Initially all the charges are unity ($n_i = \sum_s n_{is} = 1$, $n_a = \sum_s n_{as} = 1$) and this term vanishes. As V is turned on, the K atoms lose charge and this term becomes attractive. In the last line of Eq. (2), finally, the core level $E_i = E_c$ represents the Si $2p$ noninteracting level of the i th atom, which we compare with core-level photoemission experiments. In order to account for the chemical shift, an effective Coulomb repulsion, $W_c = 1.8$ eV, has been included following Riffe *et al.*²² This term describes the repulsion between the (fixed) core-level charge and the electron charge transferred, in the adsorbate process, to the valence levels

of the same Si atom.

Since the exact solution of the Hamiltonian (1) is not known, one must resort to some decoupling scheme of the two-electron terms. To be specific, we expect strong spin correlations attached to the Hubbard U term, but no significant correlation effects due to the other two-electron interactions. Therefore, the W and W_c terms will be treated just in the Hartree approximation. However, the Hubbard term cannot be disposed of so easily. Both charge and spin degrees of freedom are essential. Charge fluctuations dominate the low- U/t regime, whereas spin fluctuations overwhelmingly control the high- U/t situation. Since both may be important in the intermediate regime, it is convenient to consider them on the same footing, at least to first order. This is what unrestricted Hartree Fock (UHF) does. The on-site two-electron Green function is decoupled in terms of the one-electron Green functions as

$$\begin{aligned} \langle n_{i-s} c_{is} c_{js}^+ \rangle_\omega &= (0.5 \langle n_i \rangle - 2s \langle S_{iz} \rangle) G_{is,js}(\omega) \\ &\quad - \langle \sigma_i^{-s} \rangle G_{i-s,js}(\omega), \end{aligned} \quad (3)$$

where $S_{iz} = 0.5(n_{i\uparrow} - n_{i\downarrow})$ and $\sigma_i^{-s} = c_{i-s}^+ c_{is}$ is the deviation, or spin-flip, operator which rises (lowers) the spin for $s = -\frac{1}{2}$ ($+\frac{1}{2}$). It is just this spin-mixing term that characterizes the UHF mean-field approximation. It introduces a great deal of correlation between antiparallel-spin electrons (nondiagonal exchange), quite absent in the standard (exclusion principle) exchange of the normal Hartree-Fock approximation. This spin-mixing term, entirely alien to the original Hubbard Hamiltonian, generates a useful approximation, which satisfies all the conservation laws. Although the reliability of this approximation has never been really proved, it was used with considerable success in an analysis of possible metal-insulator transitions already in the later 1960s (Ref. 37) and, on the other hand, recent calculations^{38,39} show its usefulness even for cuprate materials with large U/t ratios. The decoupling (3) generates an effective single-particle problem in terms of average charge and spin values which must be calculated self-consistently from, e.g., the single-particle Green functions. Charge and spin correlations can then be straightforwardly computed.

III. MODELING THE INTERFACE

A proper calculation with quantitative purposes would require a careful calculation of the Si surface band structure with due consideration to the precise reconstruction at each coverage rate. Once the bulk band structure is projected out, several Si layers still remain with properties [e.g., the density of states (DOS)] different from, although rapidly approaching, their bulk values. On top of these, one or two layers of potassium atoms must be placed to simulate different coverages. Our purpose in this work, as pointed out in Sec. I, is much more modest: we shall be satisfied with semiquantitative, or even qualitative estimates. Our objective is simply to study the effect of Si on-site repulsions on the electronic structure of these interfaces. For this purpose, we introduce the

following well-defined set of simplifying assumptions.

(a) A single orbital at each site (dangling bonds at the Si atoms and s orbitals at the K atoms).

(b) All the hopping matrix elements will be scaled with distance (d) according to Harrison's rules,⁴⁰ i.e., as d^{-2} (s and p orbitals). Furthermore, the Si-K hopping integrals will be obtained by the geometric mean rule.⁴⁰ We are thus left with a single free parameter both for Si and K. The Si parameter is now adjusted so as to give a simplified bulk band structure in the gap region in the spirit of the Thorpe and Weaire Hamiltonian.⁴¹ The K parameter is likewise fitted to obtain just the lowest s band of the potassium band structure.⁴²

(c) Finally, the interatomic two-center Coulomb integrals are evaluated with Klopman's approximation⁴³

$$W_{ij} = e^2 [d_{ij}^2 + (2e^2 / (U_{ii} + U_{jj}))^2]^{-1/2}$$

in terms of the intra-atomic, one-center Coulomb integrals and the distance $d_{ij} = |R_i - R_j|$ between the two centers.

By judiciously playing with the Si-K distances, we have then been able to map the Si(100)/K interface into a *two-dimensional* extended Hubbard Hamiltonian, Eqs. (1) and (2). This approach has been used previously both for Si (Ref. 36) and GaAs (Refs. 44 and 45) interfaces. We therefore model the interface by a planar array of 24×4 Si dimers (four dimer chains) which may be symmetric or buckled and, furthermore, may be distributed in any way we choose [e.g., a $c(4 \times 2)$ pattern]. Different potassium coverages are simulated by placing the appropriate number of potassium atoms at the appropriate places. A weak interchain coupling has been allowed so as to have always a bidimensional system. Finally, periodic boundary conditions are used along both planar axes in order to keep size effects to a minimum. To avoid frustration effects, which would otherwise arise in any AF ordering, an even number of dimers is taken along the dimer rows.

Now we consider separately the initial, single-adsorbate regime, which has its own special characteristics, and higher coverages, which will be discussed afterwards.

IV. INITIAL COVERAGE: DISTORTION OF THE AF BACKGROUND

The expression initial coverage is ill-defined until some criterion is given to characterize it. We assume it really means absence of lateral interactions among the adsorbates, i.e., the single-adsorbate regime. The precise geometry of the reconstructed Si(100) surface should then, one presumes, be most important, especially in the neighborhood of the adsorption site. Neither the geometry nor the adsorption site, however, can be considered completely settled at the present time, in spite of recent experimental results,^{33,34,46} which have contributed much to clarify the situation.

Although the driving mechanism of reconstruction of the Si(100) surface, dimerization of Si atoms along the $\langle 011 \rangle$ direction, has been known for years,⁴⁷ the detailed geometry of the dimers (symmetric or asymmetric) and their distribution over the surface have been a source of

conflicting results ever since. Whereas grazing-incidence x-ray-diffraction measurements are interpreted in terms of asymmetric (buckled) dimers,⁴⁸ scanning-tunneling microscopy (STM) indicates symmetric (nonbuckled) dimers away from impurities or defects,^{49,50} and core-level shifts seem also consistent with a symmetric dimer configuration.⁵¹⁻⁵³ Other experiments are compatible with both symmetric and asymmetric dimers. Theoretical calculations, on the other hand, have also led to mutually conflicting results in this respect,^{24-27,31,32} creating their own uncertainties and disagreements.

Recently, however, Wolkow³³ has obtained STM images of dimerized Si(100) surfaces, over a wide temperature range, where buckled dimers with $c(4 \times 2)$ ordering appear at low-enough temperature (~ 120 K). Although low-temperature core-level shifts point to a substantial charge transfer between the dimers,³⁴ thus supporting the presence of buckled dimers, the situation is not so clear cut. Wolkow also observed regions of $p(2 \times 2)$ order as well as untipped (symmetric) dimer patches, in addition to a significant density of structural defects, which tend to pin nearby dimers into a buckled configuration. To complicate things a little more, an order-disorder transition leading to the disappearance of higher-order diffraction spots was predicted to take place at roughly 250 K and finally found by Tabata, Arvga, and Murata⁵⁴ in a low-energy electron-diffraction experiment [the $c(4 \times 2)$ to 2×1 phase transition at about 200 K].

We have, therefore, taken the simplest path postulating symmetric, unbuckled dimers, thus assuming high (e.g., room) temperature. However, this assumption is by no means necessary. In a very recent phenomenological model of this surface Stillinger⁵⁵ shows that a defect (e.g., an adsorbate) coupled even to a single dimer of a pattern of symmetric dimers creates a local island of anticorrelated tipping angles, i.e., the adsorbate generates a surrounding region of buckled dimers with $c(4 \times 2)$ order. This has indeed been observed in the STM work of Sakurai *et al.*⁴⁶ Hence, it should not matter much whether we start out with a (2×1) symmetric dimer

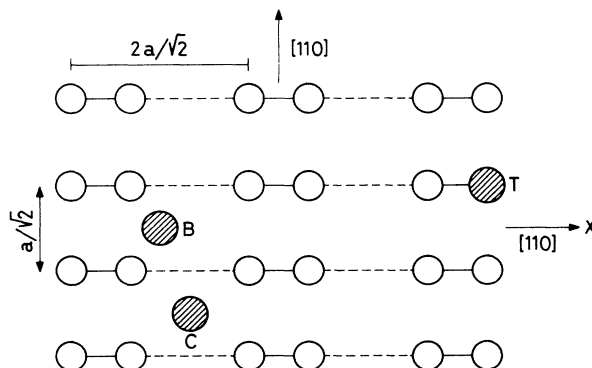


FIG. 1. Diagram of different adsorption sites (shaded circles) for potassium on the reconstructed Si(100)-(2x1) surface (empty circles) at very low coverage. *B*: off-center bridge site. *C*: cave (also called valley cave) site. *T*: top site. Lattice constant of Si: $a = 5.43$ Å.

reconstruction or with a $c(4 \times 2)$ pattern. We chose the former and place a single K atom on different adsorption sites (Fig. 1): the on-top site (T), the off-center bridge site, between two Si atoms of the same dimer row⁴⁶ (B), and finally, the cave sites (C), which will become the preferred sites for all the range of single-site occupation (up to $\theta=1$). The important point is that, for $\theta < 0.1$, the adsorbates occupy a single type of adsorption site and no higher-order diffraction spots are seen.⁴⁶

A. The Si(100)-(2×1) clean surface

Now we have a single adjustable parameter, the Hubbard U , to produce the gap we need. Figure 2 shows the expected DOS for both spins, corresponding to a Mott-Hubbard insulator (one electron per atom) with a gapwidth of 0.65 eV obtained for $U=1$ eV. The S_z on the Si atoms is ± 0.31 and the magnetic moment 0.72. The probability of double occupation has fallen from 0.25 ($U=0$) to 0.15. The Fermi level, which will be taken as reference zero energy in what follows, lies at the midpoint of the gap and is indicated by a vertical thin line.

B. Si(100)-(2×1)+1K: The charge and spin bag

Tables I and II give the distribution of charge and spin bag around a potassium atom placed in cave position, marked with K at the center of both tables. These are arranged in four double-entry columns simulating the Si atoms along the four dimer rows. The K atom transfers most of its charge (0.932 units of electron charge) to the closest four Si atoms, which are seen from Table I to have a total excess charge of 1.28 (0.32 each), clearly exceeding the transferred charge. The rest (0.35) is dragged from the surrounding Si atoms, mainly from their dimer partners (0.07 each), thus creating a neutralizing hole charge of just 0.35.

As one moves along any of the two central dimer rows, e.g., from the middle point upwards, one can see weak charge oscillations where slightly overpopulated and underpopulated dimers alternate. These dimers are, furthermore, clearly asymmetric with alternative buckling in opposite directions. The two external rows are already almost undistorted with respect to the clean surface. We thus have here another example of how, starting with symmetric dimers, rows of anticorrelated buckled dimers are induced by an adsorbate.

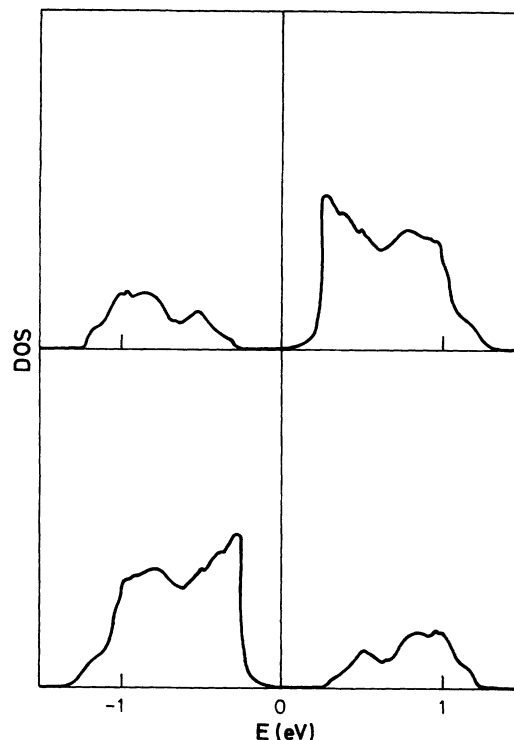


FIG. 2. Spin-resolved DOS projected on an atom of the reconstructed Si(100)-(2×1) surface, showing the Fermi level (thin vertical line) at the midpoint of the gap. Upper DOS: minority spin. Lower DOS: majority spin. The calculation has been done for a cluster of 24×4 dimers with periodic boundary conditions. A Lorentzian broadening has been used with full width at half maximum equal to the mean separation between the cluster single-particle levels.

But let us progress to the spin distribution. As Table II shows, the strong charge bag about the potassium atom is accompanied by an associated spin bag with strongly reduced S_z components whenever large deviations from unit charge in the Si atoms take place. This tends to decrease the average S_z component over the whole Si lattice, which in turn leads to a decrease of the gapwidth. We shall have something more to say below about this issue, which is at the heart of the gradual substrate metallization at higher coverage. Notice, to end

TABLE I. Total charge distribution (sum of both spins) in the Si atoms around a potassium atom (indicated by K at the center of the Table) adsorbed in the cave position on a clean Si(100)-(2×1) surface. Couples of contiguous columns simulate Si dimer rows. Although the calculation has been performed on a 24×4 dimer array, only the K-surrounding region where the charge differs from unity is shown.

0.9995	0.9995	1.0005	0.9998		0.9998	1.0005	0.9995	0.9995
0.9985	0.9985	0.9949	0.9984		0.9984	0.9949	0.9985	0.9985
0.9973	0.9973	1.0100	0.9930		0.9930	1.0100	0.9973	0.9973
0.9959	0.9959	0.9266	1.3187		1.3187	0.9266	0.9959	0.9959
0.9959	0.9959	0.9266	1.3187	K	1.3187	0.9266	0.9959	0.9959
0.9973	0.9973	1.0100	0.9930		0.9930	1.0100	0.9973	0.9973
0.9985	0.9985	0.9949	0.9984		0.9984	0.9949	0.9985	0.9985
0.9995	0.9995	1.0005	0.9998		0.9998	1.0005	0.9995	0.9995

TABLE II. Spin distribution in the Si atoms around a potassium atom (indicated by K at the center of the table) adsorbed in the cave position on a clean Si(100)-(2×1) surface. Couples of contiguous columns simulate Si dimer rows. Again only the K-surrounding region where the spin differs from its clean-surface value, 0.3113, is shown.

0.3 115	-0.3 115	0.3 103	-0.3 099	K	0.3 099	-0.3 103	0.3 115	-0.3 115
-0.3 110	0.3 110	-0.3 089	0.3 103		-0.3 103	0.3 089	-0.3 110	0.3 110
0.3 074	-0.3 074	0.2 920	-0.3 059		0.3 059	-0.2 920	0.3 074	-0.3 074
-0.3 098	0.3 098	-0.2 349	0.1 852		-0.1 852	0.2 349	-0.3 098	0.3 098
0.3 098	-0.3 098	0.2 349	-0.1 852		0.1 852	-0.2 349	0.3 098	-0.3 098
-0.3 074	0.3 074	-0.2 920	0.3 059		-0.3 059	0.2 920	-0.3 074	0.3 074
0.3 110	-0.3 110	0.3 089	-0.3 103		0.3 103	-0.3 089	0.3 110	-0.3 110
-0.3 115	0.3 115	-0.3 103	0.3 099		-0.3 099	0.3 103	-0.3 115	0.3 115

with the spin distribution, that the AF order is not really destroyed, changing only the magnitude of the S_z 's with respect to the clean surface.

The foregoing situation largely persists when the potassium atom is placed on the off-center bridge site (*B*, Fig. 1) close to a dimer row. This is then the only dimer row showing significant distortions with respect to the AF surrounding background, with a behavior quite similar to that of the central rows of the previous case. The charge transferred by the K atom is now 0.96, 0.88 going to the closest two Si atoms, which see their S_z component reduced to -0.09 . The AF ordering is still retained

throughout. When the adsorbate is placed on the top position (*T* in Fig. 1), however, something new takes place: the S_z component of the Si atom below *changes sign* ($0.31 \rightarrow -0.05$). This spin is now coupled *ferromagnetically* to the spins of its surrounding Si atoms. This has, however, an energy cost which makes this configuration higher in energy than the previous ones. The adsorbate in cave configuration has the lowest energy of all three. This spin effect is inherently tied to the existence of a Hubbard U on the Si atoms and shows a simple mechanism whereby electron correlations favor the more symmetric adsorption sites, a situation very frequent in chemisorption systems.⁵⁶

Figure 3 shows, finally, the spin-resolved DOS projected on the strongly overcharged Si atoms (full line) as well as on the K atom adsorbed on cave position (dashed line). The Fermi level jumps from its initial position in the gap (vertical thin line) to the upper Hubbard band (dashed vertical line, E_F). The potassium DOS, equal for both spins, shows a large unoccupied peak at ~ 2 eV with a small tail extending below E_F .

More interesting are the changes in the Si DOS. Comparison with Fig. 2 shows that, while the majority-spin DOS remains practically unaltered (bottom curve), the minority-spin DOS exhibits a prominent structure at the Fermi level formed essentially by a large transfer of spectral weight from the upper part of the band. There is also some spectral-weight transfer from the lower Hubbard band upwards to this E_F structure, a characteristic feature of correlated electron (or hole) -doped systems, (see, e.g., Ref. 38). Since the minority-spin charge increases while the majority-spin one remains almost constant, the S_z component is largely reduced. This is just an intuitive way of visualizing the mechanism whereby the spin bag is formed.

We want to stress that most of the fine structure in these and the rest of the DOS presented in this paper is probably a size effect due to the relatively small clusters used. Only the prominent features can be taken seriously. The small potassium peak at the Fermi level, corresponding to the Si structure just discussed, seems a real effect.

V. HIGHER COVERAGE ($0.1 < \theta < 2$) ANALYZED IN LIGHT OF THE DOUBLE-LAYER MODEL

As coverage increases, the dimer configuration becomes more symmetric while the interface is becoming

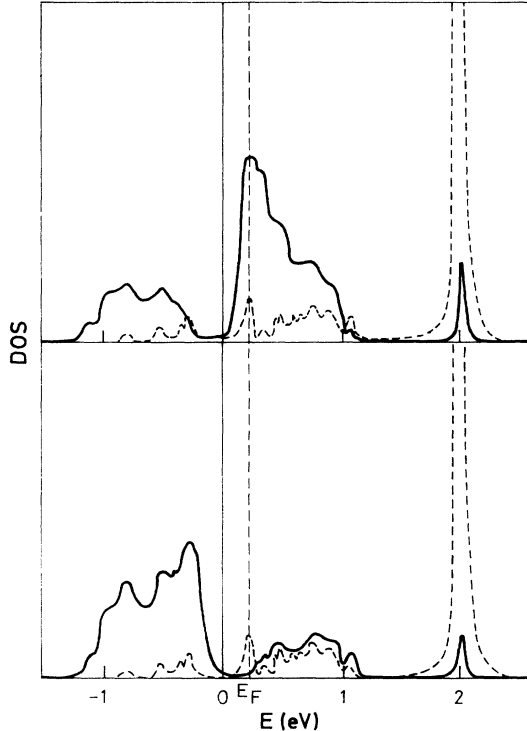


FIG. 3. Spin-resolved DOS projected on a Si atom (full line) and the adsorbate (dashed) for the independent adsorbates limit (see text) Si+1 K in cave position. The old (reference) Fermi level is indicated by the thin vertical line. Dashed vertical line: new Fermi level. Upper DOS: minority spin. Lower DOS: majority spin.

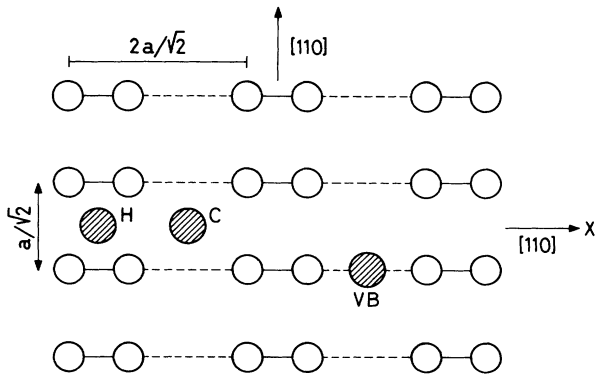


FIG. 4. Diagram of different adsorption sites (shaded circles) in the double-layer model of the alkali-covered Si(100)-(2 \times 1) surface (empty circles). *H*: pedestal site. *C*: cave site, as in Fig. 1. *VB*: valley-bridge site. *a* is the lattice constant of Si (5.43 Å).

increasingly metallic.²² As to the adsorption sites, the first single-layer model of Levine⁵⁷ was complemented by the double-layer model of Kono and co-workers,^{58,59} developed in response to the suggestion of Enta *et al.*¹⁴ that the saturation coverage seemed to be $\theta=2$, with an insulating interface. The potassium atoms were supposed to adsorb on the Levine pedestal sites (*H* in Fig. 4) until completion of the first monolayer followed, upon further coverage, by a second monolayer occupying either the cave sites (*C*) or the valley-bridge (*VB*) sites between the dimer rows. Although some experimental results^{60,61} have strongly contributed to attaining an extended consensus in favor of the double-layer model, no general agreement has been reached at the present time about the several possible combinations of first and second adsorption sites, the differences in energy being sometimes as low as 0.01 eV.⁶² For a detailed discussion of this subject, see Batra, Tekman, and Ciraci⁶³ and Kobayashi *et al.*⁶⁴ and references therein.

A. The first layer ($\theta < 1$): Substrate metallization

We place K atoms on the *C* sites of a (2 \times 1) pattern of Si-symmetric dimers. It seems that *C* sites have slightly lower binding energy than the valley-bridge sites. Figure 5 shows, for both spins, the Si and K projected local DOS (full and dashed curves, respectively), for covered parts of the surface, at different coverage in the range $0.25 < \theta < 1$. Increasing coverage is simulated by distributing the adsorbates so as to form an increasing number of chains perpendicular to the dimer rows. For $\theta=0.25$, for instance, we have a potassium chain every four dimers separated by so large a distance ($4 \times 3.84 = 15.36$ Å) that they do not interact. This is, therefore, the conventionally called "low-coverage regime," characterized by independent K chains normal to the dimers.^{46,22} The electrons lost by the K atoms go, as before, into the upper Hubbard dangling-bond band. Each potassium atom will tend to form its own charge-spin bag. However, since neighboring K atoms of the same chain are only 7.68 Å apart, their associated bags have two common di-

mers with each neighbor bag and interact so strongly that they form in fact a single bag along the potassium chain. Most of the charge transferred by the adsorbate chain is localized in this extended linear bag. When coverage increases and the K linear chains approach each other, the whole Si surface is a charge bag, i.e., metallic. This process of electron doping, similar to the doping with holes of the CuO₂ planes of a high-*T_c* superconducting material, presents also similar characteristics. (i) Since the Fermi level initially jumps through the gap into the bottom of the empty band and then rises steadily with increasing coverage, the interface would appear to metallize suddenly. However, as already explained below but now phrased differently, (ii) the AF character of the clean surface is gradually destroyed, with an accompanying decrease of the gap. The system is gradually turning metallic, but it still resembles a semiconductor with some electrons excited into the conduction band. The DOS for up and down spins are still different; (iii) the DOS for $\theta=0.25$ shows a sharp structure around the Fermi level, at the bottom of the upper Hubbard band of the minority-spin DOS (upper curves), of area increasing linearly with the number of neighbor K atoms around each Si atom. Since this structure does not appear at clean parts of the surface ($\theta=0$), it clearly accommodates the localized fraction of the transferred charge. This peak has a 0.15 4*s* K character (see below) and persists through the low-coverage range, with roughly the same composition, until the gap disappears. We identify this feature with the photoemission peak found by Enta *et al.*¹⁴, in the low-coverage region, of area linearly increasing with coverage. A sharp structure of similar characteristics is also apparent at the top of the lower Hubbard band of the majority-spin DOS (lower curve). Some spectral weight is clearly transferred by both bands into the gap region, thus reducing the Si *S_z* component (± 0.11 at $\theta=0.25$). By $\theta=0.5$ the Hubbard bands merge, and both the gap and the above peak disappear leaving just a central peak. The system is then fully metallic although still a bit spin polarized. The DOS is almost equal for both spins (*S_z* = ± 0.06), showing a three-peak structure with a dominant central peak quite reminiscent of a two-dimensional (2D) metal band. The whole structure is in agreement with the *A + C* structure observed by Soukiassian *et al.*²¹ (Fig. 2 of this reference).

Let us now look at the potassium DOS. We simply have a one-dimensional (1D) DOS at $\theta=0.25$, followed by a 2D-type DOS at $\theta=0.5$, with their corresponding Si images (small structures plotted in the full line). Since these K DOS's are mostly unoccupied, they do not imply any important adlayer metallization. This occurs at higher coverage (see below). However, the rather abrupt change in the Si DOS from 1D to 2D at $\theta=0.5$ agrees with the phase transition reported by Riffe *et al.*²² at $\theta=0.25$ (in their notation).

At $\theta=1$, finally, the spin polarization has disappeared (*S_z* = 0). We now have a fully metallic, unpolarized Si band with the Fermi level steadily rising with increasing coverage. Since we have placed K atoms on *all* cave sites, we actually have full one-dimensional potassium chains along the dimer-rows direction spaced by 7.68 Å.

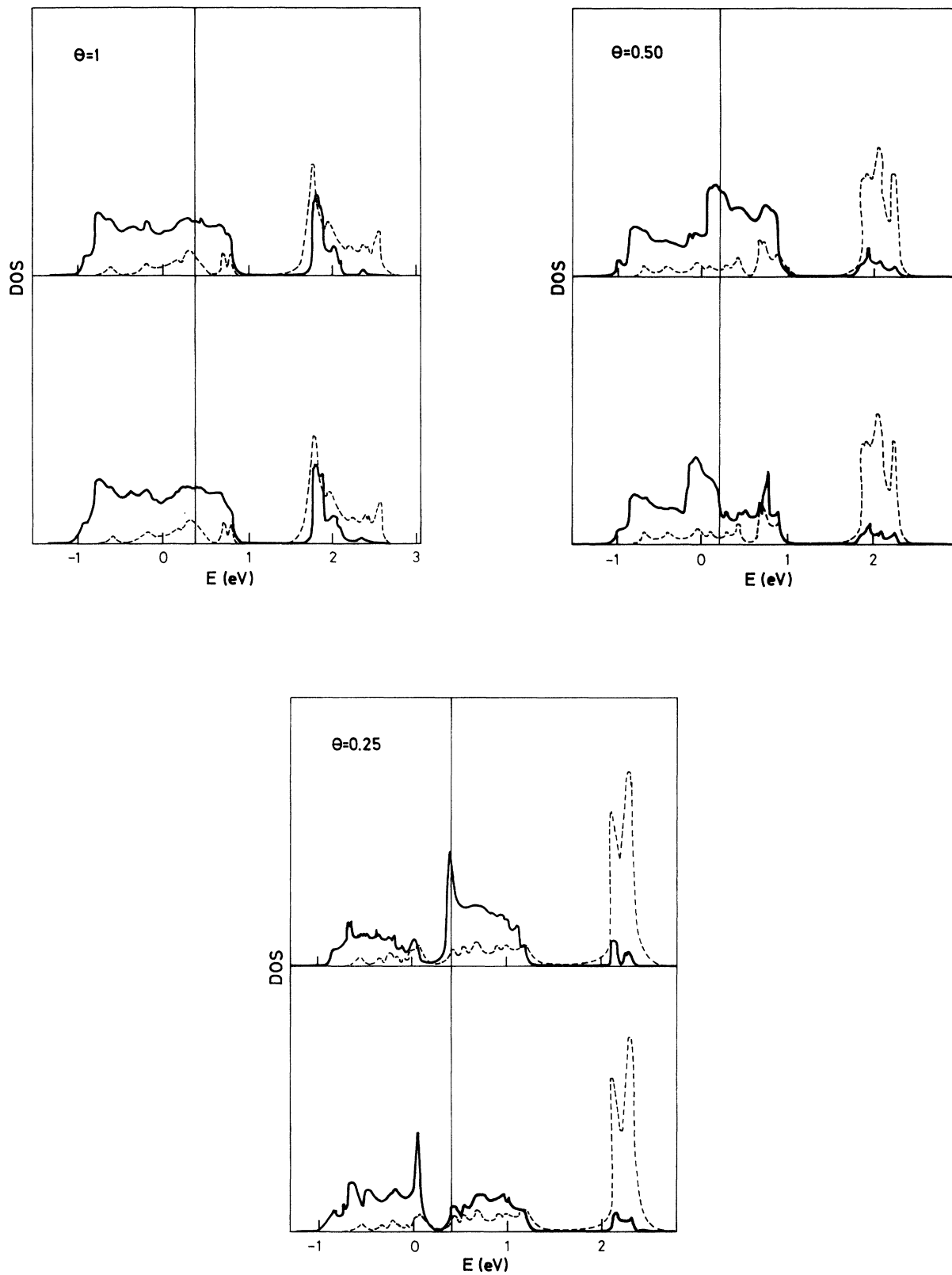


FIG. 5. Spin-resolved DOS projected on the Si (full line) and K (dashed) atoms for the potassium-covered Si(100)-(2 \times 1) surface at different coverage in the range $\theta < 1$ (the first K layer). Lower DOS: majority spin. Upper DOS: minority spin. Top-left panel, $\theta=1$. Top-right panel, $\theta=0.5$. Bottom panel, $\theta=0.25$. The Fermi level is indicated by the thin vertical line. The energy is referred to the Fermi level of the clean surface.

The strong band hopping is now within the chains (0.35 eV) which are, nevertheless, coupled by a non-negligible hopping (~ 0.1 eV). We therefore see a broad (~ 1.5 eV) 1D unoccupied potassium band superimposed on a thinner (~ 0.4 eV) 2D band at the bottom. Similar features are found in the Si band.

B. The second layer ($1 < \theta < 2$): Adsorbate metallization

Now we place a second layer occupying pedestal sites. As this layer is being covered, we simply see (Fig. 6) how the three-peak structure is gradually being filled. The Fermi level steadily rises, sweeping parts of the DOS with increasing potassium content. Reverse charge transfer, from the substrate to the adsorbate, is thus taking place. At saturation coverage ($\theta=2$), finally, the upper Hubbard band is full and the chemical potential now lies in the upper gap, below the main potassium band. The system has become a charge-transfer insulator.⁶⁵

The most important feature in this coverage regime consists now in a small peak at the top of the lower Hubbard band, which is unoccupied at $\theta=1.25$ and keeps increasing with coverage up to saturation ($\theta=2$), when it becomes rather prominent. Its potassium component

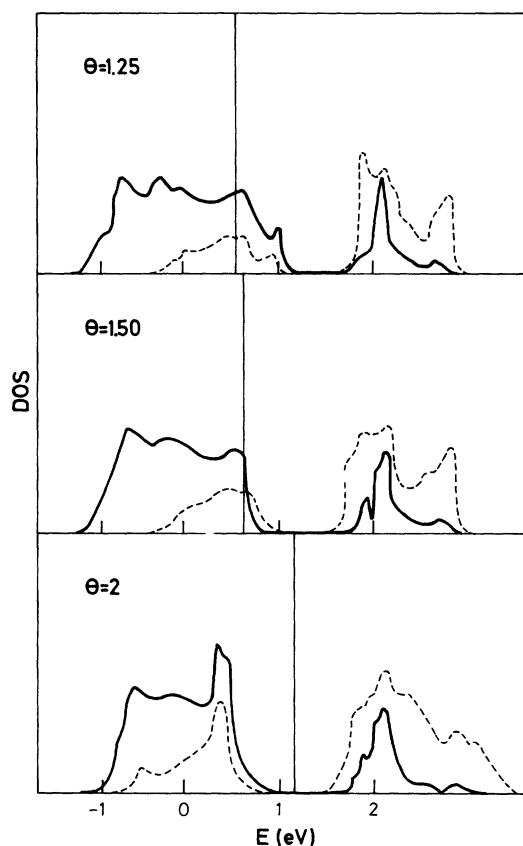


FIG. 6. Si- (full line) and K- (dashed) projected DOS for the potassium-covered Si(100)-(2 \times 1) surface in the coverage range $1 < \theta \leq 2$ (the second K layer). Since the DOS's are now equal for both spins, they are shown for one spin only. The Fermi level is indicated by the thin vertical line. The energy is referred to the Fermi level of the clean surface.

also increases and, finally, the Fermi level is crossed at $\theta=1.5$. This clearly signals a metallic potassium layer. Metallization of the K overlayer has previously been reported employing indirect experimental techniques such as energy loss^{5,6} and core-level spectroscopy,¹² as well as oxygen-dosing studies,¹⁷ but direct and conclusive evidence is also available. Nishigaki *et al.*¹⁶, using metastable de-excitation and Auger electron spectroscopies on this system, found a K 4s peak at -0.4 eV, just below the Fermi level, with growing strength from $\theta=1.48$ (in our notation) up to saturation coverage. The *s* character of this peak was attributed by these authors to hybridization between K 4s and Si dangling-bond orbitals. Johansson and Reihl¹⁹ found, in a combined direct-inverse-photoemission experiment, a potassium-derived band crossing the Fermi level just at the work-function minimum (i.e., for coverage somewhat after completion of the first layer, $\theta=1$). Effner *et al.*,¹⁸ on the other hand, found clear indication of a metallic overlayer in the stabilization of the tunneling current at saturation coverage, but they could not detect a photoemission metallic edge at saturation coverage due, perhaps, to the small photoionization cross section of the K 4s derived states at the photon energies they used (55 eV), a situation met earlier by Enta and co-workers.^{14,59}

VI. BONDING AND METALLIZATION: AN OVERVIEW

Table III and Fig. 7 display, with increasing coverage, some of the main results of this paper. The atomic charge ($q_i = \langle n_i \rangle$) is given, for Si and K, in the first two columns while the fractional ionic character (FIC) of the Si-K bond appears in the third column. The computation of this quantity requires some care since one must take into account the correct number of neighbors for each coverage. We focus attention on the most charged Si atoms in each case.

As coverage increases, Fig. 7 shows a sudden change in the slopes of the potassium charge and the FIC just after $\theta=0.5$: q_K rises from 0.09 to 0.26 and the FIC drops from 0.83 (strongly ionic) to 0.48 (moderately ionic). From $\theta=1$ up to saturation, both quantities evolve

TABLE III. Variation with coverage (θ) of different quantities for the potassium-covered Si(100)-(2 \times 1) surface. Listed are the atomic charge, $q_i = \langle n_i \rangle$, for silicon (q_{Si}) and potassium (q_K), the FIC of the adsorption bond, the Fermi level (E_F), and the apparent excess charge on the Si atoms (δq_{Si}^*).

θ	q_{Si}	q_K	FIC	E_F	δq_{Si}^*
0	1	1		0	
0.25	1.2376	0.04494	0.9012	0.2403	0.1041
0.50	1.2286	0.0856	0.8288	0.2070	0.1136
1	1.3696	0.2609	0.4783	0.4027	0.1459
1.25	1.4481	0.2831	0.4338	0.4418	0.2027
1.50	1.5162	0.3116	0.3767	0.5671	0.2011
2	1.6400	0.3600	0.2800	1.3928 ^a	0.1996

^aFor $\theta=2$, E_F lies at the midpoint of the charge-transfer gap (1.2 eV), just below the main potassium band (Fig. 6).

linearly towards their final values, 0.36 and 0.28, respectively. The Si atomic excess charge shows a minimum at $\theta=0.5$ and then also rises linearly along the rest of the coverage range up to saturation. The adsorption bond is, therefore, strongly ionic in the low-coverage regime (FIC ≈ 0.9) and predominantly covalent with rather low FIC (0.28) at saturation. The sudden drop in FIC at $\theta=0.5$ coincides with the formation of a 2D metallic overlayer, which gets increasingly hybridized and charged with increasing coverage. No special features are found after $\theta=1$. Even the crossing of the Fermi level by the peak characteristic of this coverage range, described in Sec. VB, is not reflected in any noticeable changes (apart from linear variation) in either atomic charges or FIC of the bond. It must clearly correspond to some redistribution of charge. Actually we have by now a strongly hybridized Si-K band. This is in close agreement with recent work:¹⁷ once the overlayer is metallized (for coverage about completion of the first monolayer), it remains metallic all the way up to multilayers.

The present model, however, does not sustain either the picture of the strong ionic bond along the whole coverage range^{10,20} or the small transferred charge on the Si atoms deduced from core-level experiments in the low-

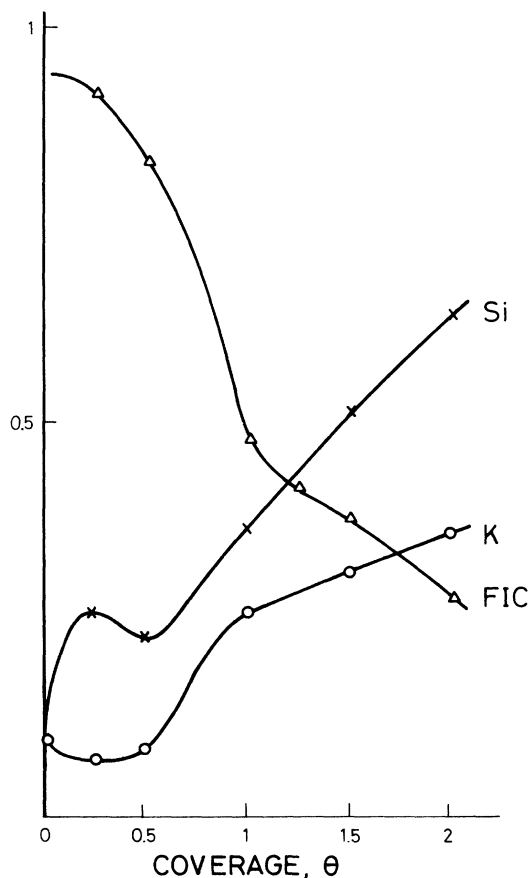


FIG. 7. Variation with coverage (θ) of the excess atomic charge on Si (crosses), potassium atomic charge (squares), and FIC of the adsorption bond (triangles) for the potassium-covered Si (100)-(2 \times 1) surface.

coverage regime.²² The first probably stems from the relative inability of the LDA to incorporate strong local-field corrections, as explained in Sec. I. Indeed the presence of active dangling bonds on the silicon surface leads to a strong energy lowering of ionic origin but, nevertheless, the on-site repulsions on the Si atoms strongly repel the arrival of a second electron, with an important drop of the double occupancy. This effect is maximum at $\theta=0.5$, just when the potassium layer is being formed and the silicon atomic charge drops to its minimum value, reflected in the steep drop of the FIC of the adsorption bond described above. Perhaps calculations based on either the GRPA (Ref. 29) or the LDA + U formalism³⁰ might cure the situation.

Concerning the core-level experiments,²² the small extra charge inferred on the Si atoms has its origin in the lack of reckoning of the appropriate Fermi level. The fourth column of Table III gives the (upward) Fermi-level shift for increasing coverage. Since the Si core-level shifts are also upwards, the core-level to Fermi-level distance is reduced, becoming somewhat insensitive to coverage. Hence, the inference that the transferred charge must be small. The apparent core-level shift δE_c^* and the apparent excess charge on the Si atoms, δq_{Si}^* , are related by $\delta E_c^* = W_c(q_s - 1) - E_F = W_c \delta q_{Si}^*$. This last quantity is listed in the last column of Table III. It ranges from 0.1 to 0.2, being clearly smaller than the real excess charges on the Si atoms, read off from the first column.

VII. CONCLUDING REMARKS

To summarize, we have studied some of the implications of an extended Hubbard model for the alkali/Si(100)-(2 \times 1) interface. A clear qualitative picture emerges from our simplified model with the following main points: (1) The insulator character of the clean Si(100) surface is explained as a simple consequence of the Hubbard model at half filling. (2) The gradual insulator-metal transition of the substrate is viewed as a gradual weakening and final destruction of the spin ordering upon doping of the surface with electron charge from the adsorbed layer. (3) In the low-coverage region (up to $\theta=0.25$), the adsorption bond is ionic and strong, with high FIC, even after the formation of 1D potassium chains perpendicular to the dimer rows. (4) At $\theta=0.5$, (one-half of the first layer), a crossover between 1D and 2D behavior is found in the adsorbate DOS signaling the onset of a potassium band which, subsequently, undergoes a rapid increase in both electron charge and hybridization with the Si band accompanied by a steep drop in the FIC of the bond. This rapid process, which seems completed at $\theta=1$, separates the low-coverage from the high-coverage regimes. (5) After completion of the first monolayer ($\theta > 1$), the above process goes on, although now slowly, along the rest of the high-coverage regime, up to saturation. In this coverage range, we find a peak which crosses the Fermi level at $\theta=1.5$ and is easily detected by metastable deexcitation spectroscopy. It is not reflected, however, in big variations of K or Si atomic charges. (6) The Fermi level of the system, which jumps across the gap of the insulator Si surface into the upper

Hubbard band at very low alkali coverages, rises steadily along this band with increasing coverage. (7) At $\theta=2$, the hybridized Si-K band is filled and the chemical potential lies in the gap below the main potassium band. The system has become a charge-transfer insulator.

ACKNOWLEDGMENTS

Financial support of the Spanish Ministry of Education and Science through DGICYT Grant No. PS90-0002 is acknowledged.

- ¹W. E. Spicer, Appl. Phys. **12**, 112 (1977); B. Reihl, V. Erbudak, and D. M. Campbell, Phys. Rev. B **19**, 6358 (1979), and references therein.
- ²S. Ciraci and I. P. Batra, Phys. Rev. Lett. **56**, 877 (1986); **58**, 1982 (1987).
- ³I. P. Batra, J. M. Nicholls, and B. Reihl, J. Vac. Sci. Technol. A **5**, 898 (1987); J. E. Northrup, *ibid.* **4**, 1404 (1986).
- ⁴U. Jostell, Surf. Sci. **82**, 333 (1979); S. A. Lindgren and L. Wallden, Phys. Rev. B **22**, 5967 (1980).
- ⁵H. Tochihara, Surf. Sci. **126**, 523 (1983).
- ⁶T. Aruga, H. Tochihara, and Y. Murata, Phys. Rev. Lett. **53**, 372 (1984); **53**, 376 (1984).
- ⁷R. V. Kasowski and M. H. Tsai, Phys. Rev. Lett. **60**, 546 (1988).
- ⁸A. U. Mc Rae, K. Muller, J. J. Lander, J. Morrison, and J. C. Phillips, Phys. Rev. Lett. **22**, 1084 (1969).
- ⁹E. Wimmer, H. Krakauer, M. Weinert, and A. J. Freeman, Phys. Rev. B **24**, 864 (1981).
- ¹⁰I. P. Batra and P. S. Bagus, J. Vac. Sci. Technol. A **6**, (1988); I. P. Batra, Prog. Surf. Sci. **25**, 175 (1987).
- ¹¹Ye Ling, A. J. Freeman, and B. Delley, Phys. Rev. B **39**, 10 144 (1989).
- ¹²E. M. Oellig, E. G. Michel, M. C. Asensio, R. Miranda, J. C. Duran, A. Muñoz, and F. Flores, Europhys. Lett. **5**, 727 (1988).
- ¹³R. Ramirez, Phys. Rev. B **40**, 3962 (1989).
- ¹⁴Y. Enta, T. Kinoshita, S. Suzuki, and S. Kono, Phys. Rev. B **39**, 1125 (1989); **36**, 9801 (1987).
- ¹⁵E. M. Oellig and R. Miranda, Surf. Sci. **117**, L947 (1986).
- ¹⁶S. Nishigaki, S. Matsuda, T. Sasaki, N. Kawanishi, Y. Ikeda, and H. Takeda, Surf. Sci. **231**, 271 (1990).
- ¹⁷E. G. Michel, P. Pervan, G. R. Castro, R. Miranda, and K. Wandel, Phys. Rev. B **45**, 11 811 (1992).
- ¹⁸U. A. Effner, D. Badt, J. Binder, T. Bertrams, A. Brodde, Ch. Lunau, H. Neddermeyer, and M. Hanbücken, Surf. Sci. **277**, 207 (1992).
- ¹⁹L. S. O. Johansson and B. Reihl, Phys. Rev. Lett. **67**, 2192 (1991).
- ²⁰I. P. Batra, Phys. Rev. B **39**, 3919 (1989).
- ²¹P. Soukiassian, M. H. Bakshi, Z. Hurych, and T. M. Gentle, Surf. Sci. **221**, L759 (1989).
- ²²M. Riffe, G. K. Wertheim, J. E. Rowe, and P. H. Citrin, Phys. Rev. B **45**, 3532 (1992).
- ²³R. I. G. Uhrberg, G. V. Hansson, J. M. Nicholls, and S. A. Flodström, Phys. Rev. B **24**, 4684 (1981); R. D. Bringans, R. I. G. Uhrberg, M. A. Olmstead, and R. Z. Bachrach, *ibid.* **34**, 7447 (1986); F. J. Himpsel and Th. Fauster, J. Vac. Sci. Technol. A **2**, 815 (1984); P. Martensson, A. Cricenti, and G. V. Hansson, Phys. Rev. B **33**, 8855 (1986).
- ²⁴D. J. Chadi, Phys. Rev. B **43**, 43 (1979).
- ²⁵J. Ihm, M. L. Cohen, and D. J. Chadi, Phys. Rev. B **21**, 4592 (1980); M. T. Yin and M. L. Cohen, *ibid.* **24**, 2303 (1981).
- ²⁶Z. Zhu, N. Shima, and M. Tsukada, Phys. Rev. B **40**, 11 868 (1989).
- ²⁷J. Dabrowski and M. Scheffler, Appl. Surf. Sci. **56**, 15 (1992).
- ²⁸J. E. Northrup, M. S. Hybertsen, and S. G. Louie, Phys. Rev. Lett. **66**, 500 (1991).
- ²⁹L. Hedin and S. Lundqvist, Solid State Phys. **23**, 1 (1969).
- ³⁰V. I. Anisimov, M. A. Korotin, J. Zaanen, and O. K. Andersen, Phys. Rev. Lett. **68**, 345 (1992).
- ³¹A. Redondo and W. A. Goddard, J. Vac. Sci. Technol. **21**, 344 (1982).
- ³²E. Artacho and F. Yndurain, Phys. Rev. Lett. **62**, 2491 (1989); Phys. Rev. B **42**, 11 310 (1990).
- ³³R. A. Wolkow, Phys. Rev. Lett. **68**, 2636 (1992).
- ³⁴E. Landemark, C. J. Karlsson, Y.-C. Chao, and R. I. G. Uhrberg, Phys. Rev. Lett. **69**, 1588 (1992).
- ³⁵J. M. López Sancho, M. C. Refolio, M. P. López Sancho, and J. Rubio, Phys. Scr. **43**, 216 (1991).
- ³⁶J. M. López Sancho, M. C. Refolio, M. P. López Sancho, and J. Rubio, Surf. Sci. **285**, L491 (1993); J. Vac. Sci. Technol. A **11**, 2483 (1993).
- ³⁷N. F. Mott, Philos. Mag. **20**, 1 (1969).
- ³⁸J. B. Grant and A. K. McMahan, Phys. Rev. Lett. **66**, 488 (1991); Phys. Rev. B **46**, 8440 (1992).
- ³⁹J. A. Vergés, F. Guinea, and E. Louis, Phys. Rev. B **46**, 3562 (1992).
- ⁴⁰W. A. Harrison, *Electronic Structure and the Properties of Solids* (Freeman, San Francisco, 1980).
- ⁴¹M. F. Thorpe and D. Weaire, Phys. Rev. B **4**, 3518 (1971).
- ⁴²D. A. Papaconstantopoulos, *Handbook of the Band Structure of Elemental Solids* (Plenum, New York, 1986).
- ⁴³G. Klopman, J. Am. Chem. Soc. **86**, 4550 (1964).
- ⁴⁴F. Flores and J. Ortega, Europhys. Lett. **17**, 619 (1992).
- ⁴⁵O. Pankratov and M. Scheffler, Phys. Rev. **70**, 351 (1993).
- ⁴⁶T. Sakurai, T. Hashizume, I. Kamiya, Y. Hasegawa, N. Sano, H. W. Pickering, and A. Sakai, Prog. Surf. Sci. **33**, 3 (1990).
- ⁴⁷R. E. Schlier and H. E. Farnsworth, J. Chem. Phys. **30**, 917 (1959).
- ⁴⁸N. Jedrecy, M. Sauvage-Simkin, R. Pinchaux, J. Massies, N. Greiser, and V. H. Etgens, Surf. Sci. **230**, 197 (1990).
- ⁴⁹R. N. Tromp, R. J. Hamers, and J. E. Delmuth, Phys. Rev. Lett. **55**, 1303 (1985).
- ⁵⁰R. J. Hamers, R. M. Tromp, and J. E. Delmuth, Phys. Rev. B **24**, 5343 (1986); R. J. Hamers and U. K. Kohler, J. Vac. Sci. Technol. A **7**, 2854 (1989).
- ⁵¹F. J. Himpsel, P. Heiman, T.-C. Chiang, and D. E. Eastman, Phys. Rev. Lett. **45**, 1112 (1990).
- ⁵²D. M. Rich, A. Samaavar, T. Miller, N. F. Lin, T.-C. Chiang, J. E. Sundgren, and J. E. Green, Phys. Rev. Lett. **58**, 579 (1987); T.-C. Chiang, in *Synchrotron Radiation in Materials Research*, edited by R. Clarke, J. Gland, and J. H. Weaver, MRS Symposia Proceedings No. 143 (Materials Research Society, Pittsburgh, 1989), p. 55.
- ⁵³D. H. Rich, T. Miller, and T.-C. Chiang, Phys. Rev. B **37**, 3124 (1988).
- ⁵⁴T. Tabata, T. Aruga, and Y. Murata, Surf. Sci. **179**, 163 (1987).

- ⁵⁵F. H. Stillinger, *Phys. Rev. B* **46**, 9590 (1992).
- ⁵⁶M. C. Refolio, J. M. López Sancho, M. P. López Sancho, and J. Rubio, *Surf. Sci.* **251/252**, 947 (1991).
- ⁵⁷J. D. Levin, *Surf. Sci.* **34**, 90 (1973).
- ⁵⁸T. Abukawa and S. Kono, *Phys. Rev. B* **37**, 9097 (1988); *Surf. Sci.* **214**, 141 (1989).
- ⁵⁹Y. Enta, S. Suzuki, S. Kono, and T. Sakamoto, *Phys. Rev. B* **39**, 5524 (1989).
- ⁶⁰M. C. Asensio, E. G. Michel, J. Alvarez, C. Ocal, R. Miranda, and S. Ferrer, *Surf. Sci.* **211/212**, 31 (1989).
- ⁶¹V. Eteläniemi, E. G. Michel, and G. Materlick, *Surf. Sci.* **251/252**, 483 (1991).
- ⁶²Y. Morikawa, K. Kobayashi, K. Terakura, and S. Blügel, *Phys. Rev. B* **44**, 3459 (1991); I. P. Batra, *ibid.* **43**, 12 322 (1991).
- ⁶³I. P. Batra, E. Tekman, and S. Ciraci, *Prog. Surf. Sci.* **36**, 289 (1991).
- ⁶⁴K. Kobayashi, Y. Morikawa, K. Terakura, and S. Blügel, *Phys. Rev. B* **45**, 3469 (1992).
- ⁶⁵J. Zaanen, G. A. Sawatzky, and J. W. Allen, *Phys. Rev. Lett.* **45**, 418 (1985).